Experimental investigation of atomic recombination in a supersonic nozzle

By CHE JEN CHEN†
Plasmadyne Corporation, Santa Ana, California

(Received 6 June 1963)

The nature of the flow of a dissociating diatomic gas in a convergent-divergent supersonic nozzle is investigated by measuring the distribution of flow parameters along the nozzle. Two parameters are measured, namely the degree of dissociation and the static pressure. The degree of dissociation is measured by a spectroscopic method. The pressure is measured by U-tube manometers. The results are compared with Bray's (1959) theory and Logan's (1957) prediction.

1. Introduction

The flow of a dissociating gas through a convergent-divergent nozzle has recently been the subject of intensive study, which includes relaxation phenomena of different degrees of freedom of different species, and interactions between the different species. These relaxation phenomena have been studied by many authors; among them Krieger (1951), Penner (1955), Logan (1957), Heims (1958), Bray (1959), and Kushida (1960). Particularly interesting results were obtained by Logan and Bray. Logan applied linearized theories, similar to those that were derived by Penner, to atomic recombination in a hypersonic wind tunnel. He predicted that, in a hypersonic nozzle, the lack of equilibrium would occur in the early part of the nozzle because dT/dt is largest at that region. Equilibrium is regained at a later stage of expansion by a release of dissociation energy. Bray used the ideal-dissociating-gas concept of Lighthill (1957) and Freeman (1958) to set up the equations of one-dimensional motion. Assuming a simple reaction rate equation, together with a number of different values for the reaction rate constant, the equations were solved numerically. He was able to calculate the flow parameters at different points along the nozzle for different values of the rate constants, and could predict the deviation from chemical equilibrium that would occur in the nozzle for a very wide range of rate constant. Once such a deviation has begun, he showed that the gas will 'freeze', and the dissociation fraction will remain almost constant if the flow is expanded further.

The present experimental work is concerned with the measurement of the pressure distribution and degree of dissociation of a diatomic gas flowing through a convergent-divergent supersonic nozzle. The theoretical values of the flow parameters are calculated following Bray's method for two conditions: namely,

---

† Present address: Jet Propulsion Laboratory, California Institute of Technology, Pasadena, California.

the reaction-rate constant equal to zero (frozen flow), and the rate constant assumed to be infinite (equilibrium flow). The experimental distribution of the flow parameters are compared with the calculated ones to determine the nature of the flow. It is hoped that this work will shed some light on the verification of the proposed theories, especially that formulated by Bray (1959) and Logan (1957).

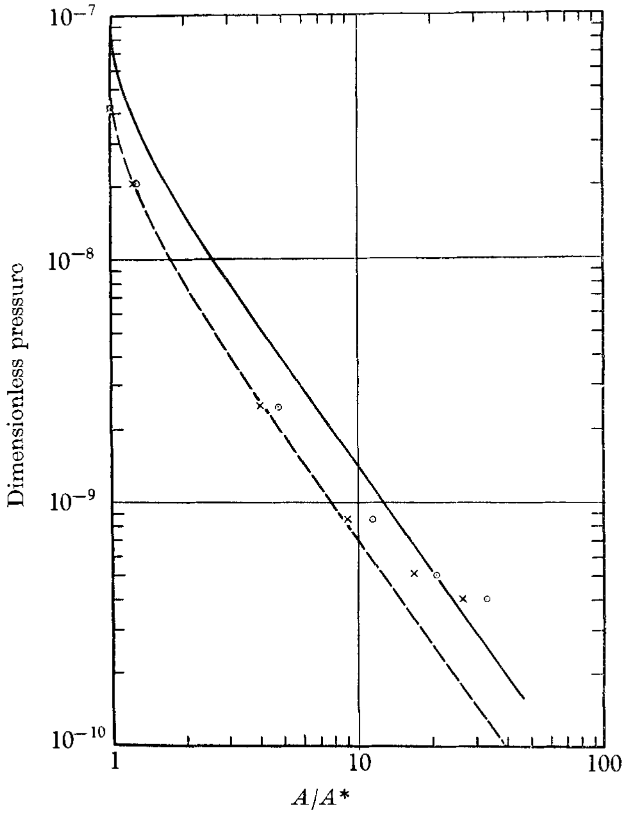

FIGURE 1. Dimensionless pressure versus area ratio for hydrogen flow in supersonic nozzle. ⊙, Experimental points before boundary-layer correction; ×, experimental points after boundary-layer correction; ———, theoretical equilibrium flow, $\Phi \rightarrow \infty$; – – – –, theoretical frozen flow, $\Phi \rightarrow 0$; mixing chamber condition: pressure = 25·1 cm Hg, enthalpy = 23,800 B.Th.U./lb.

2. Theoretical background and calculations

The Bray (1959) theory was applied with a conventional arc-jet in mind. This jet is made of an arc chamber, a mixing chamber and a conical nozzle. Equilibrium conditions prevail in the mixing chamber because of the long residence time of the gas particles in the chamber compared with the relaxation time. Thus, the initial conditions for the nozzle flow can be derived from a measurement of pressure and enthalpy in the mixing chamber. If the initial conditions are known, Bray's formulations can be solved for hydrogen gas with two extreme conditions; when Bray's reaction rate parameter $\Phi \rightarrow 0$ for frozen flow and $\Phi \rightarrow \infty$ for equilibrium flow.

The results of the calculations made for hydrogen are given in dimensionless representations in figures 1–4 for two typical sets of initial conditions.

One of Bray's important conclusions is that when frozen flow has occurred in the nozzle, it cannot reverse toward equilibrium.

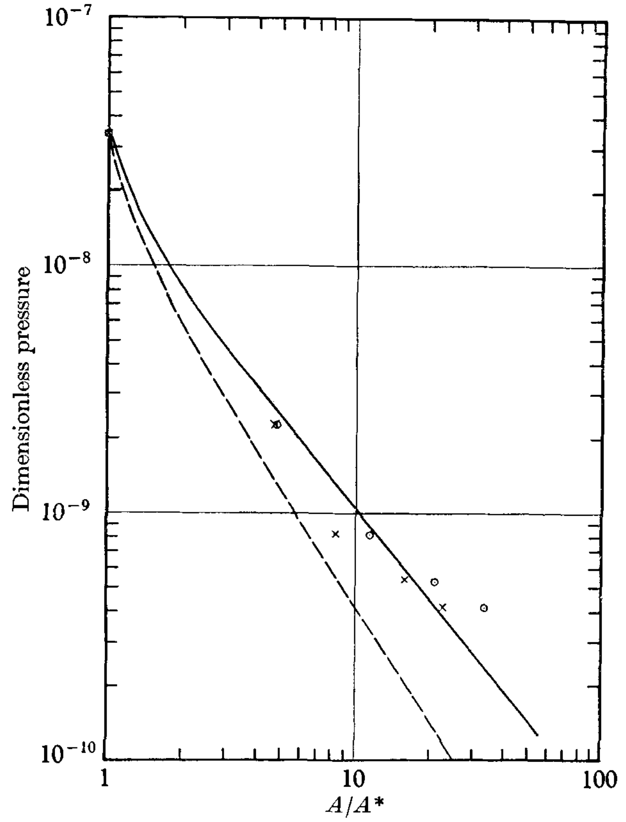

FIGURE 2

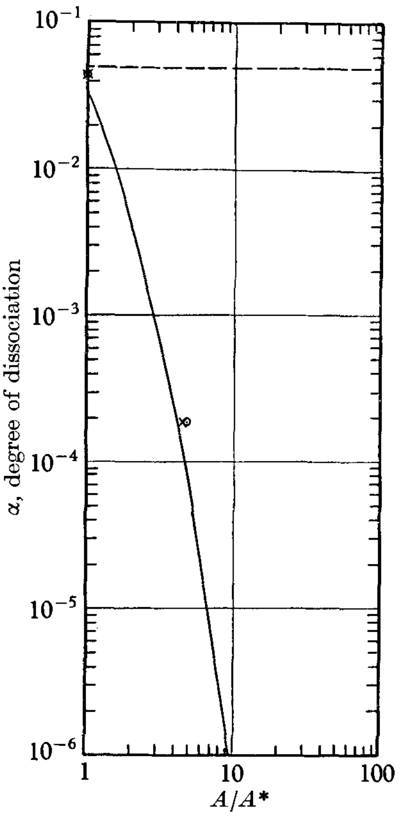

FIGURE 3

FIGURE 2. Dimensionless pressure versus area ratio for hydrogen flow in supersonic nozzle. ⊙, Experimental points before boundary-layer correction; ×, experimental points after boundary-layer correction; ———, theoretical equilibrium flow, $\Phi \to \infty$; – – – –, theoretical frozen flow, $\Phi \to 0$; mixing chamber condition: pressure = 20·0 cm Hg, enthalpy = 60,200 B.Th.U./lb.

FIGURE 3. Degree of dissociation versus area ratio for hydrogen flow in supersonic nozzle. ⊙, Experimental points before boundary-layer correction; ×, experimental points after boundary-layer correction; ———, theoretical equilibrium flow, $\Phi \to \infty$; – – – –, theoretical frozen flow, $\Phi \to 0$; mixing chamber condition: pressure = 25·1 cm Hg, enthalpy = 23,800 B.Th.U./lb.

Logan (1957) applies Penner's (1955) approach in a hypersonic wind tunnel. He concludes that the effects of lag in the chemical reaction can be assessed by comparison of a reciprocal characteristic time for flow process, $T^{-1}(dT/dt)$, with the relaxation times, the characteristic times for adjustment of the reactions. He has derived a criterion for the flow to remain near equilibrium. It is

$$\frac{1}{T}\frac{dT}{dt}\tau \leqslant 10^{-3}, \qquad (1)$$

where τ is the maximum value of the reaction time for the chemical process, i.e. the time for the concentration to reach a value $(1-e^{-1})$ times the equilibrium concentration, t is time, and T is temperature. According to equation (1), the lack of equilibrium will occur in the early part of the nozzle where dT/dt is large. This nearly frozen-flow region will be followed by an adjustment zone wherein equilibrium is regained by a sudden irreversible release of the dissociation energy and with a large increase of entropy accompanying a considerable reduction of the Mach number in the nozzle.

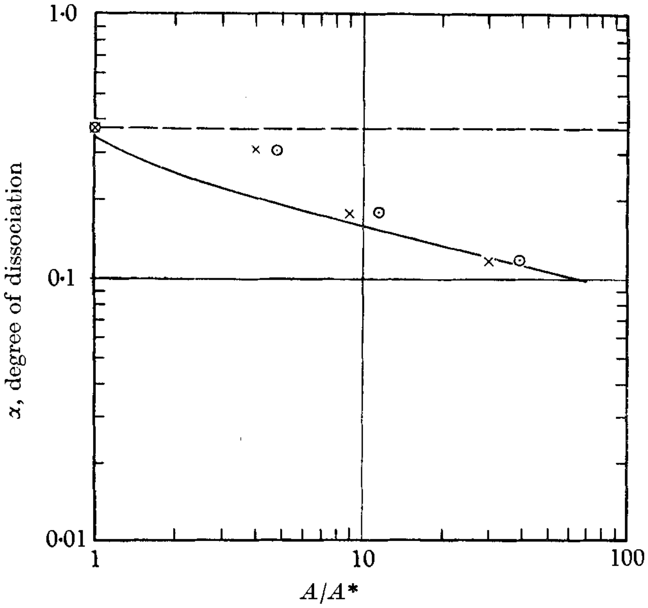

FIGURE 4. Degree of dissociation verus area ratio for hydrogen flow in supersonic nozzle. ⊙, Experimental points before boundary-layer correction; ×, experimental points after boundary-layer correction; ———, theoretical equilibrium flow, $\Phi \to \infty$; – – – –, theoretical frozen flow, $\Phi \to 0$; mixing chamber condition: pressure = 20·0 cm Hg, enthalpy = 60,200 B.Th.U./lb.

3. Experimental methods

3.1. *Gas source and nozzle design*

The apparatus used for the experiments is shown schematically in figure 5. The nozzle is a simple conical configuration with the following dimensions: diameter of throat, 0·25 in.; diameter of exit, 1·54 in.; length from throat to exit, 8·51 in.; half angle, 4° 20′; area ratio at exit, 37·9: 1.

The nozzle is made of copper and can be cooled by running water through the jacket. The nozzle cone angle was chosen so that the area gradient along the axis of the cone would be small, and thus the flow would be expected to be nearly one-dimensional. A Plasmadyne Plasmatron M-4 is used to heat the gas. It is a d.c. electric-arc discharge device through which gas flows from an independent gas supply. It creates high temperatures and can be run with various gases, such as air, N_2, H_2, A, and He. The power input can reach 150 kW. Both positive and negative electrodes, which are made of copper with tungsten lining, are water-cooled. The impurity in the flow due to the electrode corrosion was measured and found to be less than 0·5 %. The highest enthalpies obtainable vary with the gas used; for air, for example, it is about 20,000 B.Th.U./lb. In the present experiments the enthalpies of the gases are so adjusted that the gases are appreciably dissociated while the ionization effect can be ignored.

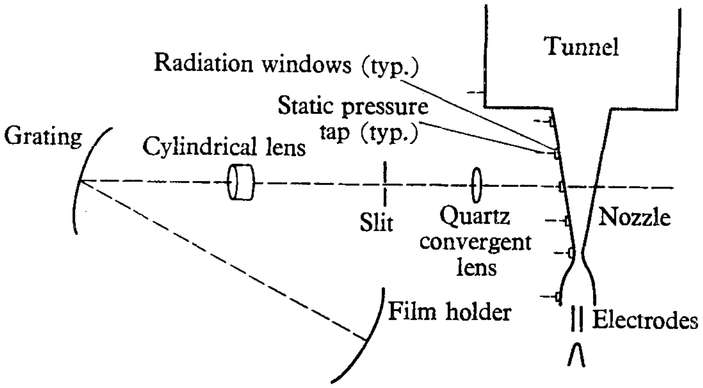

FIGURE 5. Schematic diagram of apparatus.

Five groups of viewing windows are provided on the side wall of the nozzle. They are equally spaced along the nozzle axis. Each group is made of windows equally spaced along a tangent to the cone cross-section, thus providing the possibility of survey through different portions of the cross-section. The number of windows in each group varies from a single opening at the throat to five at the exit, according to the diameter of the nozzle at the various group locations. The diameter of each window is 0·079 in. The windows are made of synthetic sapphire, a product of the Linde Company, New York.

3.2. *Pressure measurement*

The instrument selected for pressure measurements is the simple U-tube manometer, with either mercury or silicon oil as the working fluid. The manometers used for measuring the pressure in the mixing chamber and at the throat are filled with mercury; the other manometers are filled with silicon oil. One side of each manometer is connected to a fore-pump which can evacuate to a pressure of the order of 10μ of mercury. With such arrangements the pressure measurement error can be kept below 2 %.

3.3. *Spectrographic measurement*

A spectroscopic technique can be used to identify the species in the flow and also to obtain the degree of dissociation. The relative abundances of the hydrogen atoms to the hydrogen molecules can be deduced from the ratio of the intensity of a hydrogen atomic line to that of a hydrogen molecular spectrum (or secondary spectrum) in the following manner.

The intensity of a spectral line originating from a certain species can be expressed (Finkelnburg 1950) as

$$I = \frac{h\nu F g}{z} N e^{-\epsilon/kT}, \tag{2}$$

where I is the intensity of the line, h the Planck constant, ν the frequency, g the statistical weight, F the transition probability, z the partition function, N the number density, ϵ the upper energy state, k the Boltzmann constant, and T the temperature. The ratio of the line intensities originating from species a and b will be

$$\frac{I_a}{I_b} = \frac{\nu_a F_a g_a z_b N_a}{\nu_b F_b g_b z_a N_b} \exp - \left(\frac{\epsilon_a - \epsilon_b}{kT}\right). \tag{3}$$

If the two lines are generated by transitions from upper energy states having approximately the same energy values, then equation (3) becomes

$$\frac{I_a}{I_b} = \frac{\nu_a F_a g_a z_b N_a}{\nu_b F_b g_b z_a N_b}. \tag{4}$$

In case the lines are observed at different positions along the nozzle the only variables at the right-hand side of equation (4) are N and z. z is a function of temperature; but for moderate temperature ranges such as we have (~ 2000–6000 °K), z can be considered a constant without introducing appreciable error. Under this assumption, equation (4) can be written

$$\frac{N_a}{N_b} = K\frac{I_a}{I_b}, \tag{5}$$

where K is a constant, standing for

$$\frac{\nu_b F_b g_b z_a}{\nu_a F_a g_a z_b}.$$

Now, the dissociation reaction of a diatomic molecule can be expressed as

$$H_2 = H + H, \tag{6}$$

and the degree of dissociation, α, is defined by

$$\alpha = \frac{N_H}{N_H + 2N_{H_2}}. \tag{7}$$

Combining equations (5) and (7) and choosing species a as the dissociated atoms, and species b as the undissociated molecules, we find

$$\frac{N_a/N_b}{N_a/N_b + 2} = \frac{K(I_a/I_b)}{K(I_a/I_b) + 2}. \tag{8}$$

The value of K can be determined by using suitable initial conditions; for example, in our case the conditions in the mixing chamber can be measured and α can be calculated by using the Saha equation. Then K can be obtained by measuring I_a/I_b in the mixing chamber. Once K has been determined, α can be determined anywhere along the nozzle through the use of equation (8) and the locally measured value of I_a/I_b. The method described is particularly useful in the case of hydrogen for two reasons. First, the rotational spectrum of H_2 is made of distinct lines. This feature renders the intensity measurement easier. Also, there are a few H_2 lines in the visible region which have upper energy levels very close to the strong hydrogen atomic lines H_α, H_β, H_γ and H_δ; for example, H_δ has an upper energy of 13·154 eV, and the hydrogen molecular line 5615·6 Å has the value 13·164 eV.

The percentage error introduced into the above procedure by assuming $\epsilon_a = \epsilon_b$ can be estimated as follows:

$$\frac{I_a}{I_b} = c\exp\{-(\epsilon_a - \epsilon_b)/kT\} \approx c\left[1 - \frac{\epsilon_a - \epsilon_b}{kT}\right]. \tag{9}$$

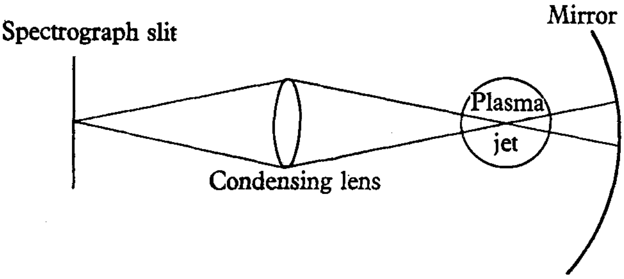

FIGURE 6. Diagram of apparatus for absorption measurement.

Now kT is of the order of 0·5 eV, so that percentage error will be

$$\frac{13{\cdot}164 - 13{\cdot}154}{0{\cdot}5} \times 100 = 2\,\%.$$

If the gas is not optically thin, the emitted radiation may be reabsorbed. Lines of a given element radiate out through the absorbing fringe, where elements of the same kind may absorb some of this radiation, thereby causing a weakening of the emitted intensity. The amount of self-absorption increases rapidly with concentration of absorbing vapour. The relationship between I_0, the intensity of the emitted radiation and I_1, the intensity after some absorption is

$$I_1 = I_0 e^{-\sigma l},$$

where l is the path distance and σ is the absorption coefficient. For given operating conditions, the intensity of a line is the most important factor in determining the absolute amount of self-absorption. The next most important factor is the lowness of the lower energy level of the line. Higher intensity and lower level lines suffer more in self-absorption. To measure the opacity of the gas, a cylindrical mirror was placed coaxially with the gas jet on the side opposite the spectroscope. Spectrograms were taken with and without the mirror in position. The corresponding ratios of the intensities of the lines, in both cases, were compared and absorption coefficients calculated. The apparatus arrangement is shown in figure 6.

The spectrograph used was a 1·5 meter, Model No. 11, Bausch and Lomb grating type instrument with the following specifications. Spectrum coverage: 1st order, 3700–7800 Å; 2nd order, 1850–3700 Å. Dispersion: 1st order, 15 Å/mm; 2nd order, 7·5 Å/mm. The instrument used for the identification of lines and the measurement of intensities was the Model 2250 Comparator and Densitometer designed by Applied Research Laboratories. The wavelength can be read to 0·01 Å, and the error in intensity measurement is estimated to be less than 5 %. The film is conventionally calibrated by step neutral filters covering the different wavelengths of interest.

3.4. *Experimental procedure and boundary-layer correction*

The enthalpy of the gas is controlled by the mass flow and the electrical input power delivered to the arc head. For a stable operating point at a specified enthalpy, the relation between the mass flow, voltage and current is rather critical. A series of trial runs had to be made to determine the best running conditions. The surface condition of the nozzle inner wall plays an important role in the nozzle flow pattern, and it was necessary to clean and polish it carefully before each run.

The pressure in the mixing chamber was measured directly with a manometer attached to that chamber. The enthalpy in the mixing chamber was found by subtracting cooling losses to the arc head and nozzle from the total electric input power and dividing by the mass flow rate of gas through the arc chamber.

The displacement thickness of the boundary layer in the nozzle was calculated by using the method proposed by Cohen & Reshotko (1955). This is an approximate method for the calculation of the compressible laminar boundary layer with heat transfer and arbitrary pressure gradient, with the major restriction that the linear viscosity law is valid. The effective area ratio calculated is presented in figures 1–4.

4. Experimental results

4.1. *Static pressure*

The static pressure measurements obtained from two typical hydrogen runs are plotted on figures 1 and 2 for comparison with theory.

4.2. *Determination of the degree of dissociation*

The hydrogen atomic Balmer line H_β (4101·735 Å) and hydrogen molecular line (5615·6 Å) were identified using the iron reference spectrum. The relative line intensities were measured using the densitometer. The results are plotted on figures 3 and 4 for comparison with theory. A correction has been made to take care of the quenching effects due to reabsorption by the 'mirror, or no mirror' experiment. This correction changes the final data by as much as 35 %.

5. Comparison of theory and experiment

Figures 1–4 show that the experimental flow is not frozen all the way to the nozzle exit. Rather, it is shifting from the frozen flow condition incurred early in the expansion towards equilibrium flow near the exit. According to Bray's theory for the present geometrical configuration and the stagnation conditions, the flow should be equilibrium at the early stage of expansion and shift suddenly to frozen flow at somewhere in the nozzle at a later stage of expansion. On the other hand, Logan (1957) has studied the relaxation phenomena in a nozzle by assuming that a departure from equilibrium will occur in regions where the rate of change of temperature is large. If Bray's approach is used to calculate dT/dt for $\Phi \to 0$ (because of a lack of accurate data on τ for hydrogen, the criterion (1) cannot be calculated), the results indicate that dT/dt near the throat is about one order of magnitude higher than that near the exit. The nearly frozen flow near the throat, as the experimental results indicated, is followed by an adjustment zone wherein equilibrium is regained by a sudden irreversible release of the dissociation energy, with a large increase of entropy and reduction of the Mach number in the nozzle. The temperature and density (ρ) changes along the nozzle lag behind the ideal isentropic flow. These lags can be approximated by

$$T' - T'' = (dT'/dt)\tau,$$
$$\rho' - \rho'' = (d\rho'/dt)\tau,$$

where the double prime quantities are the local actual values. T'' and ρ'' are, respectively, larger than T' and ρ' because both dT'/dt and $d\rho'/dt$ are negative. The fact that the temperature and density are larger than the equilibrium values will cause a decrease in the relaxation time which, according to Wood (1956), is inversely proportional to the square root of the temperature and the square of the density. The decrease of the relaxation time and Mach number (increasing the time of flight of the gas particles) has the effect of shifting the flow toward equilibrium. The general trend of these experimental results appears to agree with Logan's prediction.

The author wishes to express his gratitude to Mr J. Rosener, for his constant interest and encouragement. He also wishes to thank Dr D. A. Russell for his helpful discussion, Mr Robert Price for his help with the numerical calculations, and Mr Edwin Myers for his assistance in some measurements. This work is supported by NASA under contract No. NAS 8-844.

REFERENCES

Bray, K. N. C. 1959 *J. Fluid Mech.* **6**, 1.
Cohen, C. B. & Reshotko, Eli 1955 *Nat. Adv. Comm. Aero., Wash., Tech. Rep.* no. 1294.
Finkelnburg, W. 1950 *Atomic Physics.* New York: McGraw-Hill Book Co.
Freeman, N. C. 1958 *J. Fluid Mech.* **4**, 4.
Heims, S. P. 1958 *Nat. Adv. Comm. Aero., Wash., Tech. Note* no. 4144.
Krieger, F. J. 1951 *Amer. Rocket Soc. J.* **21**, 179.
Kushida, R. 1960 *Liquid Rockets and Propellants.* p. 385. Ed. L. E. Bollinger, etc. New York: Academic Press.
Lighthill, M. J. 1957 *J. Fluid Mech.* **2**, 1.
Logan, J. G. 1957 *Inst. Aero. Sci., Wash.,* Preprint no. 728.
Penner, S. S. 1955 *Chemical Reaction in Flow System.* London: Butterworth.
Wood, G. 1956 *Nat. Adv. Comm. Aero., Wash., Tech. Note* no. 3634.